Physics Letters B 807 (2020) 135528

Contents lists available at ScienceDirect

Physics Letters B

www.elsevier.com/locate/physletb

Two-step description of heavy ion double charge exchange reactions

Jessica I. Bellone [a], Stefano Burrello [a], Maria Colonna [a,*], José-Antonio Lay [b,c], Horst Lenske [d]

NUMEN Collaboration

[a] INFN-LNS, I-95123 Catania, Italy
[b] Departamento de FAMN, Universidad de Sevilla, Apartado 1065, E-41080 Sevilla, Spain
[c] Instituto Interuniversitario Carlos I de Física Teórica y Computacional (iC1), Apdo. 1065, E-41080 Sevilla, Spain
[d] Institut für Theoretische Physik, Justus-Liebig-Universität Giessen, D-35392 Giessen, Germany

ARTICLE INFO

Article history:
Received 29 November 2019
Received in revised form 27 March 2020
Accepted 29 May 2020
Available online 3 June 2020
Editor: J.-P. Blaizot

Keywords:
Heavy ion reaction theory
Double charge exchange reactions
Theory of nuclear charge exchange excitations
Double beta decay

ABSTRACT

Heavy ion double charge exchange reactions are described by sequential meson-exchange, corresponding to a double single charge exchange (DSCE) reaction mechanism. The theoretical formulation is discussed. The fully quantum mechanical distorted wave 2-step calculations are shown to be reproduced very well by approximating the intermediate propagator by its pole part. The role of ion-ion elastic interactions is discussed. As a first application, calculations are performed for the reaction ^{40}Ca(^{18}O, ^{18}Ne)^{40}Ar at 15 AMeV. Results are compared to the data measured at LNS by the NUMEN Collaboration. Formal analogies between the nuclear matrix elements (NME) involved in DSCE reactions and in double β-decay are pointed out.

1. Introduction

Nuclear double charge exchange (DCE) reactions are of large current interest after it was realized that they give access to a hitherto hardly explored sector of nuclear excitations. In early DCE studies, the focus was on aspects of the dynamics of proton and neutron pair transfer [1,2] which at that time was thought to be the dominant reaction mechanism of heavy ion DCE scattering. About a decade later, Blomgren et al. [3] attempted to measure the double-Gamow-Teller resonance (DGTR) in a heavy ion DCE reaction which, however, at that time was not successful. Only recently, it was realized that under appropriate conditions DCE reactions are the perfect tool for spectroscopic nuclear structure investigations [4,5], being also of high interest for the nuclear structure aspects underlying exotic weak interaction processes. That change of paradigm relies on the observation that under appropriate conditions isovector nucleon-nucleon (NN) interactions will be the driving forces, thus extending the longstanding experience with single charge exchange (SCE) reactions [6–9] to higher order processes. By obvious reasons, that conjecture can be explored the best by peripheral coherent reactions with complex nuclei, leading to ejectiles with particle-stable $\Delta Z = \pm 2$ final states. A distinct advantage of heavy ion scattering over the former (π^+, π^-)-DCE reactions [10–12] is the much easier experimental availability and handling of ion beams.

In this work, we propose a new reaction mechanism for peripheral heavy ion DCE reactions at energies well above the Coulomb barrier. We investigate the conditions under which such reactions can be described as a double single charge exchange (DSCE) process, driven by collisional NN interactions, thus extending our investigations in Refs. [13,14] to higher order processes. We will not consider transfer DCE which, in fact, has been found to be negligible for the reactions considered here [15,16]. A formalism is developed for the description of DCE reactions by two consecutive $\Delta Z = \pm 1$ SCE steps. In a DCE reaction, however, the SCE processes are contributing off-the-energy shell as intermediate processes. Hence, their description requires special attention. An important point is the proper treatment of the strongly absorptive elastic ion-ion interactions for which we use a microscopic optical model potential. The spectroscopic aspects are described by Hartree-Fock-Bogoliubov (HFB) and Quasiparticle Random Phase (QRPA) theory following the microscopic approach presented in [13].

* Corresponding author.
E-mail addresses: jessica.bellone@ct.infn.it (J.I. Bellone), burrello@lns.infn.it (S. Burrello), colonna@lns.infn.it (M. Colonna), lay@us.es (J.-A. Lay), horst.lenske@theo.physik.uni-giessen.de (H. Lenske).

https://doi.org/10.1016/j.physletb.2020.135528

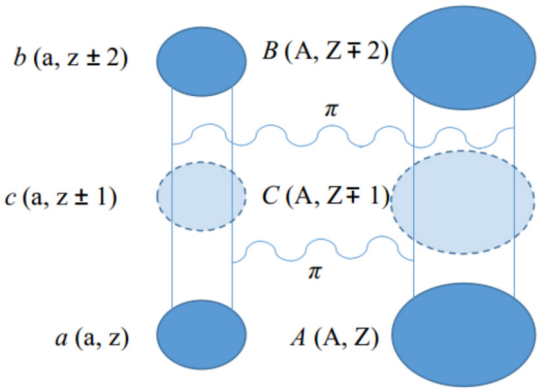

Fig. 1. Schematic representation of a two-step double charge exchange transition as two consecutive single charge exchange processes.

As a further new aspect, we explore the prospects for linking nuclear matrix elements (NME) extracted from DCE cross sections to NME of second order weak processes. We will show that the DCE reaction amplitudes have a striking formal similarity to the NME of $2\nu2\beta$ decay. While the latter are rare events, heavy ion DCE reactions can be studied suitably under well defined laboratory conditions. In particular, the feasibility of measuring a heavy ion DCE reaction has been recently proved, on the example of the reaction ^{18}O $+^{40}$Ca $\rightarrow ^{18}$Ne $+^{40}$Ar at E/A = 15 AMeV, indeed hinting towards a direct mechanism [17]. A complication to be dealt with in a DCE reaction is the convolution of the SCE spectra of the intermediate projectile- and target-like nuclei. Since that occurs at half off-shell conditions, the knowledge of the corresponding on-shell SCE cross sections is only of limited advantage. On the theoretical level, the problem is well under control as will be seen by the results discussed below, although inevitably hampered by a certain degree of model dependence – as is true for SCE reactions with light and heavy projectiles as well. For SCE reactions, however, appropriate methods are already available for the extraction of single–beta decay NME [13,18–21].

The paper is organized as it follows: In section 2 the theoretical framework for DSCE reactions is presented. Two practical descriptions for cross section evaluations are discussed which emphasize different aspects of sequential DCE reactions. Results of numerical calculations for the afore mentioned reaction ^{18}O $+^{40}$Ca $\rightarrow ^{18}$Ne $+^{40}$Ar are discussed in section 3. In section 4 we break down the reaction amplitude into a form displaying explicitly the connections to double β-decay. The paper closes with a summary, conclusions, and an outlook in section 5.

2. Theoretical framework of DSCE reactions

2.1. General aspects of two-step DCE reactions

The formalism developed here applies to heavy ion DCE reactions of the kind

$$ {}^{a}_{z}a + {}^{A}_{Z}A \rightarrow {}^{a}_{z\pm2}b + {}^{A}_{Z\mp2}B \tag{1} $$

with special emphasis on the collisional NN-mechanism.

The reaction, leading from the entrance channel $\alpha = \{a, A\}$ to the exit channel $\beta = \{b, B\}$, changes the charge partition by a balanced redistribution of protons and neutrons. The two reaction partners are acting mutually as the source or sink, respectively, of the charge-transferring virtual meson fields, as depicted in Fig. 1.

The differential DCE cross section is defined as

$$ d\sigma_{\alpha\beta} = \frac{m_\alpha m_\beta}{(2\pi\hbar^2)^2}\frac{k_\beta}{k_\alpha}\frac{1}{(2J_a+1)(2J_A+1)} \times \sum_{\substack{\mathcal{M}_a,\mathcal{M}_A\in\alpha \\ \mathcal{M}_b,\mathcal{M}_B\in\beta}} \left| M^{DCE}_{\alpha\beta}(\mathbf{k}_\alpha,\mathbf{k}_\beta)\right|^2 d\Omega, \tag{2} $$

where $\mathbf{k}_\alpha$ ($\mathbf{k}_\beta$) denotes the relative 3-momentum and m_α (m_β) is the reduced mass. $\{J_a\mathcal{M}_a, J_A\mathcal{M}_A\cdots\}$ and $\{J_b\mathcal{M}_b, J_B\mathcal{M}_B\cdots\}$ account for the full set of (intrinsic) quantum numbers specifying the initial and final channel states, respectively.

The DCE reaction mechanism is assumed as a sequence of two uncorrelated SCE events, each one mediated by the action of the isovector NN-interactions, acting between projectile and target and leading to pn^{-1} and np^{-1} particle-hole excitations or vice versa, respectively. After the first SCE event the system propagates undisturbed until the second interaction. Thus, the reaction proceeds as a double single charge exchange process, which by the number of separate projectile-target interactions is a two-step reaction [22,23].

The reaction matrix element, connecting incident and final channels is readily written down as a quantum mechanical amplitude in distorted wave approximation (DWA):

$$ \mathcal{M}^{DSCE}_{\alpha\beta}(\mathbf{k}_\alpha,\mathbf{k}_\beta) \approx \langle \chi^{(-)}_\beta, bB|\mathcal{T}_{NN}\mathcal{G}\mathcal{T}_{NN}|aA, \chi^{(+)}_\alpha\rangle, \tag{3} $$

corresponding to second order perturbation theory in the residual charge-transferring interaction T_{NN} but being non-perturbative in the initial state (ISI) and final state (FSI) ion-ion interactions. The latter are accounted for, to all orders, by the distorted waves $\chi^{(\pm)}_{\alpha,\beta}(\mathbf{r})$ with asymptotically outgoing and incoming spherical waves, respectively.

The anti-symmetrized nucleon-nucleon T-matrix $\mathcal{T}_{NN}$ was discussed in breadth in [13]. Central and rank-2 tensor interactions are included, covering the full spectrum of spin-independent Fermi-type ($S = 0, T = 1$) and spin-dependent Gamow-Teller-type ($S = 1, T = 1$) operators of all multipolarities.

The off-shell propagation of the system in the intermediate $\Delta Z = \pm1$ channels is described by the full many-body Green's function $\mathcal{G}$, expanded in terms of the eigenstates of the intermediate projectile-like (c) and target-like (C) nuclei as

$$ \mathcal{G} = \sum_{\gamma=cC} |cC\rangle G^{(+)}_\gamma(\omega_\alpha)\langle cC|. \tag{4} $$

The relative motion degrees of freedom are described by the channel Green's functions with asymptotically outgoing spherical waves

$$ G^{(+)}_\gamma(\omega_\alpha) = \int \frac{d^3k_\gamma}{(2\pi)^3}|\chi^{(+)}_\gamma\rangle\frac{1}{\omega^{(+)}_\alpha - \omega_\gamma}\langle\tilde{\chi}^{(+)}_\gamma| \tag{5} $$

where $\omega^{(+)}_\alpha = \omega_\alpha + i0+$ is located in the upper half of the complex plane, see e.g. [24]. The energy denominator depends on the total centre-of-mass energies of the system in the entrance and intermediate channels, respectively. In non-relativistic notation, we have

$$ \omega_\alpha = M_a + M_A + \frac{k^2_\alpha}{2m_\alpha} \qquad \omega_\gamma = M_c + M_C + \frac{k^2_\gamma}{2m_\gamma}, \tag{6} $$

where $\omega_\alpha = \sqrt{s_\alpha}$ is fixed by the Mandelstam variable s_α. M_a, M_A (and M_c, M_C) denote the nuclear masses in the initial and intermediate channel, the latter including excitation energies. $\mathbf{k}_\gamma$ indicates the (off-shell) relative momentum in the intermediate channel.

The Green function is given by a bi-orthogonal set of distorted waves $\chi^{(\pm)}_\gamma$ and their dual counterparts $\tilde{\chi}^{(\pm)}_\gamma$ [24], accounting

properly for the elastic ion-ion-interactions with diffractive and strongly absorptive potential components.

We apply to the right hand side of the Eq. (5) the completeness relation

$$\int |\tilde{\chi}_\gamma^{(-)}\rangle \frac{d^3k_\gamma}{(2\pi)^3}\langle\chi_\gamma^{(-)}| = 1 \tag{7}$$

and use

$$\langle\tilde{\chi}_\gamma^{(+)}|\tilde{\chi}_\lambda^{(-)}\rangle = (2\pi)^3\tilde{S}_\gamma^\dagger(\mathbf{k}_\gamma)\delta_{\gamma\lambda}\delta(\mathbf{k}_\gamma - \mathbf{k}_\lambda) \tag{8}$$

where $\tilde{S}_\gamma$ is the dual S-matrix associated with the hermitian conjugate channel Hamiltonian, i.e. with a creative optical potential. Thus, the channel propagator becomes

$$G_\gamma(\omega_\alpha) = \int \frac{d^3k_\gamma}{(2\pi)^3}|\chi_\gamma^{(+)}\rangle \frac{\tilde{S}_\gamma^\dagger(\mathbf{k}_\gamma)}{\omega_\alpha^{(+)} - \omega_\gamma}\langle\chi_\gamma^{(-)}|. \tag{9}$$

Inserting Eq. (9) into Eq. (3), the DSCE transition matrix element reads

$$\mathcal{M}_{\alpha\beta}^{DSCE}(\mathbf{k}_\alpha, \mathbf{k}_\beta) = \sum_{\gamma=c,C}\int \frac{d^3k_\gamma}{(2\pi)^3}$$
$$\times\mathcal{M}_{\gamma\beta}^{SCE}(\mathbf{k}_\gamma, \mathbf{k}_\beta)\frac{\tilde{S}_\gamma^\dagger(\mathbf{k}_\gamma)}{\omega_\alpha^{(+)} - \omega_\gamma}\mathcal{M}_{\alpha\gamma}^{SCE}(\mathbf{k}_\alpha, \mathbf{k}_\gamma) \tag{10}$$

showing that the DCE transition amplitude can be expressed as superposition of reaction amplitudes $\mathcal{M}_{\alpha\gamma}^{SCE}$ and $\mathcal{M}_{\beta\gamma}^{SCE}$, into and out of the intermediate channels γ, respectively.

2.2. The convolution approach

The Cauchy principal value parts of the DSCE amplitudes have the tendency to be suppressed because of compensating positive and negative contributions. To a good approximation, they can be neglected and we may evaluate the convolution integral of the two SCE amplitudes in Pole Approximation (PA), amounting to project the modulus k_γ to its on-shell value, defined by $\omega_\gamma = \omega_\alpha$:

$$\mathcal{M}_{\alpha\beta}^{DSCE}(\mathbf{k}_\alpha, \mathbf{k}_\beta) \approx -i\pi\sum_{\gamma=c,C} k_\gamma m_\gamma$$
$$\times\int \frac{d\Omega_\gamma}{(2\pi)^3}\mathcal{M}_{\gamma\beta}^{SCE}(\mathbf{k}_\gamma, \mathbf{k}_\beta)\tilde{S}_\gamma^\dagger(\mathbf{k}_\gamma)\mathcal{M}_{\alpha\gamma}^{SCE}(\mathbf{k}_\alpha, \mathbf{k}_\gamma). \tag{11}$$

This kind of approach maintains the character of the DCE reaction as a sequence of two independent SCE reactions. In PA the reaction amplitude displays that property by the convolution of two on-shell SCE amplitudes which, in principle, are accessible in SCE reactions. However, in practice this would mean to identify SCE transitions up to very high excitation energies.

As seen below, Eq. (11), leads to an astonishingly good reproduction of the full two-step DWA cross sections. However, for the sake of a deeper insight into the essentials of the DSCE reaction mechanism, further reductions are extremely valuable. For example, additional steps are necessary for the extraction of spectroscopic information out of measured cross sections, because from Eq. (11) the relation of the DSCE reaction amplitude to projectile and target nuclear matrix elements is not immediately clear. A caveat is the presence of initial state and final state interactions.

In order to quantify those effects a separation of elastic ion-ion interactions and nuclear structure effects is helpful. In momentum representation, the SCE amplitudes are given as [13]

$$\mathcal{M}_{\alpha\gamma}^{SCE} = \int d^3p\mathcal{N}_{\alpha\gamma}(\mathbf{p}, \mathbf{k}_\alpha, \mathbf{k}_\gamma)\mathcal{U}_{\alpha\gamma}^{SCE}(\mathbf{p}) \tag{12}$$

and for the second SCE amplitude accordingly. The transition potential $\mathcal{U}_{\alpha\gamma}^{SCE} = \langle\varphi_{\mathbf{k}'}, cC|\mathcal{T}_{NN}|aA, \varphi_{\mathbf{k}}\rangle$ corresponds to the reaction amplitudes evaluated with plane waves $\varphi_{\mathbf{k}}$ and $\mathbf{p} = \mathbf{k} - \mathbf{k}'$. Their structure for central interactions is

$$\mathcal{U}_{\alpha\gamma}^{SCE}(\mathbf{p}) = \sum_{S=0,1,T=1} V_{ST}^{(C)}(p^2)$$
$$\times\langle c|\mathcal{R}_{ST}(\mathbf{p}, 1_a)|a\rangle\cdot\langle C|\mathcal{R}_{ST}(\mathbf{p}, 2_A)|A\rangle, \tag{13}$$

where the bilinear forms of one-body operators [13]

$$\mathcal{R}_{ST}(\mathbf{p}, k) = e^{i\mathbf{p}\cdot\mathbf{r}_k}(\boldsymbol{\sigma}_k)^S(\boldsymbol{\tau}_k)^T, \tag{14}$$

acting in projectile (k =1) or target (k = 2), respectively, have been introduced. Expressions for rank-2 spin-tensor interactions are found in [13]. The connection of the transition potentials to nuclear matrix elements will be discussed in section 4.

Elastic ion-ion interactions are accounted for by the distortion coefficient

$$\mathcal{N}_{\alpha\gamma}(\mathbf{p}, \mathbf{k}_\alpha, \mathbf{k}_\gamma) = \frac{1}{(2\pi)^3}\langle\chi_\gamma^{(-)}|e^{i\mathbf{p}\cdot\mathbf{r}}|\chi_\alpha^{(+)}\rangle$$

which can be considered as a half off-shell extension of the S-matrix, approaching in the plane wave (PW) limit $\mathcal{N}_{\alpha\gamma}^{(PW)} = \delta(\mathbf{p} + \mathbf{k}_\alpha - \mathbf{k}_\gamma)$. In [13], the distortion coefficients were investigated in detail for SCE reactions. For the present case, it is important that $\mathcal{N}_{\alpha\gamma}$ can be decomposed into a forward component, given by an absorption factor $n_{\alpha\gamma}$ and a residual distortion form factor which we neglect in the following. Hence, we use in forward scattering approximation

$$\mathcal{N}_{\alpha\gamma}(\mathbf{k}_\alpha, \mathbf{k}_\gamma) \simeq n_{\alpha\gamma}\delta(\mathbf{p} + \mathbf{k}_\alpha - \mathbf{k}_\gamma). \tag{15}$$

That leads in Eq. (10) to a product of two distortion residues and the dual S-matrix. The absorptive effects from the intermediate channels are cancelled to a large extent by the dual S-matrix which allows to replace the product of the two distortion coefficients and the dual S-matrix by the residue $N_{\alpha\beta} = \langle n_{\gamma\beta}\tilde{S}_\gamma^\dagger n_{\alpha\gamma}\rangle_\gamma$, appropriately averaged over the intermediate channels. Thus, at low momentum transfer the DSCE amplitude is given approximately by

$$\mathcal{M}_{\alpha\beta}^{DSCE}(\mathbf{k}_\alpha, \mathbf{k}_\beta) \approx N_{\alpha\beta}(\mathbf{k}_\alpha, \mathbf{k}_\beta)\sum_{\gamma=c,C}$$
$$\times\int \frac{d^3k_\gamma}{(2\pi)^3}\mathcal{U}_{\gamma\beta}^{SCE}(\mathbf{k}_\gamma - \mathbf{k}_\beta)\frac{1}{\omega_\alpha - \omega_\gamma + i\eta}\mathcal{U}_{\alpha\gamma}^{SCE}(\mathbf{k}_\alpha - \mathbf{k}_\gamma) \tag{16}$$

by which one can separate nuclear and reaction dynamics. This expression can be reduced further by the pole approximation as in Eq. (11). Finally, Eq. (16) implies that, at small momentum transfer, ISI and FSI effects are restored into the matrix elements by replacing the PW amplitudes $\mathcal{U}_{\kappa\lambda}^{SCE}$ by amplitudes evaluated with distorted waves in the incoming α and the outgoing β channel, but retaining the plane waves in the intermediate channels γ.

2.3. The separation approach

In this section, an approach is presented which allows the separation of the DCE reaction amplitude into a nuclear structure and a reaction part by exploiting the distorted wave completeness relation. That requires to go somewhat deeper into the multipole structure of DCE reaction amplitudes. The SCE transition form factors, expressed in coordinate representation, as a function of the distance between projectile and target centres of mass, read:

$$F_{\alpha\gamma}(\mathbf{r}) = \sum_{S=0,1}\langle cC|V_{ST}^{(C)}(\boldsymbol{\sigma}_a\cdot\boldsymbol{\sigma}_A)^S\boldsymbol{\tau}_a\cdot\boldsymbol{\tau}_A|aA\rangle \tag{17}$$

They are expanded into multipole form factors

$$F_{\alpha\gamma}(\mathbf{r}) = \sum_{\lambda\mu}\sum_{\lambda_c\lambda_C} A_{S\lambda}^{\lambda_c\lambda_C} F_{(S\lambda_c\lambda_C)\lambda\mu}(\mathbf{r}) \tag{18}$$

where angular momentum coupling coefficients involving the nuclear spins are not shown explicitly, but for which we refer to Ref. [13]. The A-coefficients contain the remaining coupling of the projectile and target multipoles (λ_c and λ_C, respectively) to the resulting total angular momentum transfer λ with projection μ. The form factors are parameterized in terms of transition amplitudes $\beta_{S\lambda_k}$ and reduced form factors of unit transition strength:

$$F_{(S\lambda_c\lambda_C)\lambda\mu}(\mathbf{r}) = \left[\beta_{S\lambda_c}^{ac}\beta_{S\lambda_C}^{AC}\right] U_{S\lambda\mu}(\mathbf{r}), \tag{19}$$

as practised successfully in the Multi Step Direct Reaction (MSDR)-theory of [27–29]. For practical purposes, it is useful to define the coupled spectroscopic amplitudes

$$\beta_{S\lambda}^{ac,AC} = \sum_{\lambda_c\lambda_C} A_{S\lambda}^{\lambda_c\lambda_C}\beta_{S\lambda_c}^{ac}\beta_{S\lambda_C}^{AC} \tag{20}$$

With corresponding expressions for the second step form factor, the summation over the intermediate states leads to the spectroscopic densities

$$\rho_{\lambda_1\lambda_2}^{S_1S_2}(\omega_\alpha, k_\gamma) = \sum_{cC} \frac{\beta_{S_2\lambda_2}^{cb,CB}\beta_{S_1\lambda_1}^{ac,AC}}{\omega_\alpha^{(+)} - M_c - M_C - k_\gamma^2/2m_\gamma} \tag{21}$$

In the energy denominator, we replace k_γ by an average value $\bar{k}$. By this manipulation, the propagator and the k_γ–integration are decoupled. The latter leads to the DW completeness relation in the intermediate channel, so that the reaction amplitude becomes

$$\mathcal{M}_{\alpha\beta}^{DSCE} \approx \sum_{S_1\lambda_1\mu_1, S_2\lambda_2\mu_2} \rho_{\lambda_1,\lambda_2}^{S_1S_2}(\omega_\alpha, \bar{k}) \times\langle\chi_\beta^{(-)}|U_{S_2\lambda_2\mu_2}U_{S_1\lambda_1\mu_1}|\chi_\alpha^{(+)}\rangle. \tag{22}$$

An irreducible representation is obtained by further coupling the two reduced form factors to total angular momenta. Thus, the DCE process is described by a reduced DWA reaction amplitude fully accounting for the reaction dynamics. The two-step character of the DCE process leads to the special kind of form factor. The nuclear structure aspects of the sequential DCE process are contained in the spectroscopic density combining the SCE response of projectile and target. The β-amplitudes are related to the reduced beta-decay matrix elements in the same way as known from the so-called collective model for inelastic scattering [24]. Theoretically, they are fixed by the nuclear SCE response functions as fractions of multipole sum rules which in parallel determine also the reduced form factors $U_{S\lambda\mu}$ [27–29].

3. Results

3.1. Numerical details

The theory is of general applicability without constraints neither on the kind of transition nor on the multipolarity.

The nuclear ingredients are obtained on the basis of the Giessen EDF (GiEDF) approach [25,26] with Hartree Fock Bogolubov (HFB) ground state densities and on top of them charged current QRPA (ccQRPA) calculations. In the reaction calculations, microscopic optical potentials are used. They were obtained by folding the HFB one-body ground-state densities of projectile and target with the isoscalar and isovector parts of the (anti-symmetrized) NN T-matrix of Ref. [30]. As discussed in [13,14] ccQRPA calculations are performed to evaluate the SCE projectile and target transition densities. The projectile and target transition form factors were obtained by folding the ccQRPA transition densities with the central and rank-2 tensor parts of the anti-symmetrized NN T-matrix of Ref. [30]. All folding calculations were done in momentum representation.

Two kinds of reaction calculations were performed: The full partial wave two-step formalism, as discussed e.g. in [27–29], was used in solving the set of inhomogeneous scattering equations by direct numerical integration, as available by the computer code FRESCO [31]. These results serve as benchmark calculations for the approximations discussed in section 2. In parallel, independent calculations using the perturbation theoretical formalism were performed: Single charge exchange form factors, the DWA reaction amplitudes and the corresponding cross sections were calculated by our standard DWA-SCE computer code package HIDEX [32]. As found in Ref. [13], the calculation of the SCE reaction amplitudes requires a quite involved angular momentum algebra to couple the intrinsic nuclear angular momenta to the resulting total orbital angular momentum, by which the multipolarity observed at the level of the cross section is determined. In general, one finds

$$\mathcal{M}_{\alpha\beta}^{SCE}(\mathbf{k}_\alpha, \mathbf{k}_\beta) = \sum_{\ell_\alpha,\ell_\beta;\ell m} C_{J_aJ_AJ_bJ_B}^{\ell_\alpha\ell_\beta\ell} \times M_{\ell_\alpha\ell_\beta\ell}(k_\alpha, k_\beta)\left[Y_{\ell_\alpha}(\Omega_\alpha)Y_{\ell_\beta}(\Omega_\beta)\right]_{\ell m} \tag{23}$$

where the C-coefficients describe the recoupling of nuclear spins $J_{a,b}$ and $J_{A,B}$, respectively, to the angular momenta ℓ acting in the ion-ion relative motion sector. The situation simplifies, however, for the DCE $(0_a^+, 0_A^+) \to (0_b^+, 0_B^+)$ case as here. Then, the transitions into and out of the intermediate states necessarily must proceed through the same kind of multipolarity ℓ, leading to a total angular momentum transfer L = 0. In particular, for $(0_a^+, 0_A^+) \to (0_b^+, 0_B^+)$ transitions, the total angular momentum transfer in projectile and target $\mathbf{J}_{P,T} = \mathbf{L}_{P,T} + \mathbf{S}_{P,T}$ is constrained to $J_{P,T} = 0$ where each of the angular momenta is the (vectorial) sum of the angular momenta of the first and second transition. This allows a total spin transfer of $S_{P,T} = 0, 2$ and consequently $L_{P,T} = 0, 2$. Finally, projectile and target always combine to a total spin transfer $S = 0$ and, correspondingly, to a total angular momentum transfer L = 0.

3.2. The reaction $^{18}O + ^{40}Ca \to ^{18}Ne + ^{40}Ar$

As an illustrative application, we consider the data available for the reaction ^{18}O $+^{40}$Ca $\to^{18}$Ne $+^{40}$Ar at $T_{lab} = 270$ MeV, which has been the object of recent experimental investigations [17]. We focus on the simplest case, namely $0_{gs}^+ \to 0_{gs}^+$ transitions both in projectile and target. The intermediate channels of this DCE reaction are defined by the odd-odd nuclei ^{18}F and ^{40}K, which are both of a quite complex spectroscopic structure: rather dense spectra with a number of high-spin levels are observed close to $^{18}F(1^+, g.s.)$ as well as in close vicinity to $^{40}K(4^-, g.s.)$. A detailed survey of the corresponding spectra and their rather successful description by our ccQRPA is found in [13,14]. Here, the ccQRPA spectral distributions and transition densities for $^{18}O(0^+, g.s.) \to {}^{18}F(J^\pi, E_x)$ and $^{40}Ca(0^+, g.s.) \to {}^{40}K(J^\pi, E_x)$ are used to calculate form factors, transition potentials, and the SCE reaction amplitudes.

We start following the convolution approach. For the sake of simplicity, to check the quality of our calculations and to investigate the relevance of the distortion effects, we first include only one single intermediate channel. In particular, we consider the transition with total angular momentum and parity transfer $J^\pi =$

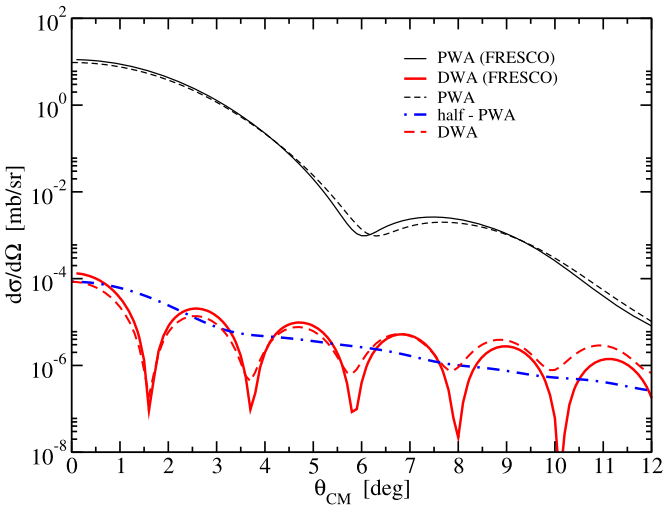

Fig. 2. Angular distribution of the differential cross section for the DCE reaction $^{18}O + ^{40}Ca \rightarrow ^{18}Ne + ^{40}Ar$ at 15 AMeV, as obtained within PWA (black thin lines) and DWA (red thick lines). Only one intermediate channel is considered (see text). Our simulations (dashed lines) are compared to the results of the FRESCO code (full lines). The dot-dashed blue curve refers to an hybrid calculation with plane waves in the intermediate channel, thus modelling the separation approach, Eq. (16).

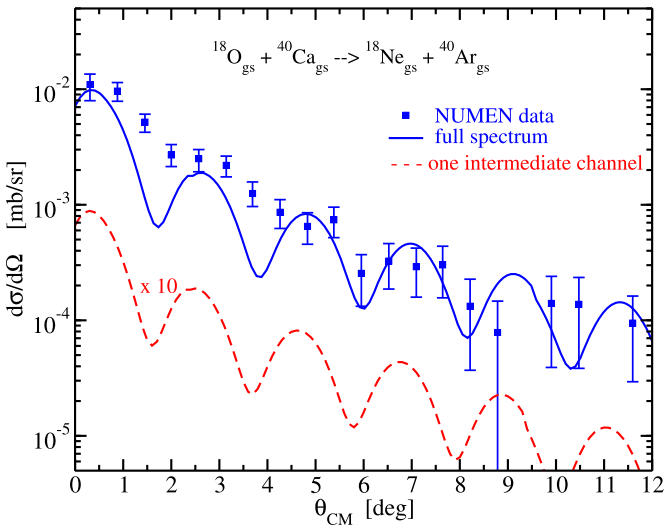

Fig. 3. Experimental angular distribution for the DCE reaction $^{18}O_{gs} + ^{40}Ca_{gs} \rightarrow ^{18}Ne_{gs} + ^{40}Ar_{gs}$ at 15 AMeV [17] compared with DSCE calculation performed with only one intermediate state (red dashed line), and considering the full virtual intermediate state integration (blue full line). Both cross sections are folded with the experimental angular resolution ($\Delta\theta_{exp} = 0.6°$).

1^+ for both projectile and target nuclei, leading to the ground state of ^{18}F and to the first excited 1^+ state at $E_x = 2.29$ MeV of ^{40}K. These states correspond to the Gamow-Teller transitions discussed in Ref. [13]. The SCE amplitudes were used to construct the second order integral of Eq. (11) which was evaluated numerically. An instructive exercise is to compare results of calculations in plane wave approximation (PWA) and in DWA, giving insight on the effects of elastic ion-ion interactions in DCE reactions. In Fig. 2 we show the angular distributions obtained by second order PWA and DWA calculations for the reaction considered.

That figure contains a number of important messages for future research on heavy ion DCE reactions. First of all, ISI and FSI effects suppress cross sections by many orders of magnitudes as a result of the strong absorption, showing that $|N_{\alpha\beta}|^2 \sim 10^{-5}$. As discussed in [13], the quenching will increase rapidly with increasing target and/or projectile mass. The suppression decreases with incident energy which, however, at realistically accessible energy scales hardly compensates the mass-dependent quenching. One can also observe that our numerical calculations, based on Eq. (11), i.e. adopting the PA (dashed lines), reproduce quite well the FRESCO results (full lines).

The results show a strong influence of the optical model potentials on the diffraction structure of angular distributions, superimposing those reflecting the reaction form factor properties. In Fig. 2, this is realized by comparing the DWA results (dashed red line) to the results which were obtained considering plane waves in the intermediate channel (dot-dashed blue line). The latter calculation is able to reproduce the DWA cross section at very small angles, but exhibits a quite flat angular distribution. These results indicate both the virtue and the limitations of the scaling approach, Eq. (16): At vanishing momentum transfer, the magnitude of the full DWA two-step cross section is rather well described, but the scaling approach is unable to account for the diffraction structure at larger momentum transfer, thus restricting that kind of approach to forward angles.

We now move to discuss the results obtained considering an extended spectrum of intermediate states. We have taken into account intermediate transitions up to $E_x = 15$ MeV and $0^{\pm} \leq J^{\pi} \leq 5^{\pm}$, for both ^{18}F and ^{40}K, using the ccQRPA results discussed in Ref. [13]. In total, the DCE spectrum includes the mixture of double $S_1 = S_2 = 0$ (non-spinflip) and $S_1 = S_2 = 1$ (spinflip) transitions (where the indices 1 and 2 refer to first and second step, respectively), both coupled to total $S = 0$ when combining projectile and target. The calculations include rank–2 tensor interactions. According to the considered J^{π} range, several multipolarities can be excited in the intermediate state, for both projectile and target, provided they are compatible with the DCE $0^+ \rightarrow 0^+$ transition in both nuclei. It has been checked that our choice leads to convergent results. Calculations have been performed following the (more easy to handle) formalism provided by Eq. (22), where energy conservation has been imposed to determine the average value $\bar{k}$.

Results are shown in Fig. 3 and compared to the NUMEN experimental data, where the theoretical angular distributions were folded with the experimental angle resolution. The DWA results of Fig. 2, with only one intermediate state, are also shown for comparison. By the inclusion of the full spectrum of intermediate channels, the calculations come close to the data without additional adjustment. The shape of the angular distribution is dominated by the $L = 0$ characteristics. The diffraction structure of the DWA angular distributions is more pronounced than observed experimentally. Also, a slight apparent underestimation of the data at certain forward angles is seen. Since we can exclude admixtures of transfer processes, with all care, these remaining discrepancies may indicate contributions of processes of an origin different from the DSCE reaction mechanism, e.g. the two-nucleon scenario discussed in [14].

4. Analogies to double β–decay

We emphasize that the DSCE theory introduced above is a suitable approach for the quantitative description of (sequential) DCE reactions. This microscopic approach is self–contained in the sense that nuclear structure and reaction dynamics are described in a fully compatible manner. The same nuclear structure will enter of course into calculations of NME for single and double beta–decay matrix elements – which, however, is not an issue for this letter. The aim of this section is to elucidate the connections of DSCE theory to nuclear spectroscopy on a more formal level and to point more explicitly to the physics content.

The ccQRPA calculations are done by the polarization propagator method which amounts to avoid setting up large matrices but solves the Dyson–equation for the QRPA–Green function – as

used for the SCE investigations in [13]. Within that formalism and the convolution approach, the reaction amplitude, Eq. (16), can be written as:

$$\mathcal{M}^{DSCE}_{\alpha\beta}(\mathbf{k}_\alpha, \mathbf{k}_\beta) \approx$$
$$N_{\alpha\beta} \sum_{SS'} \int \frac{d^3k_\gamma}{(2\pi)^3} \Gamma^{(C)}_{SS'}(\mathbf{q}_{\gamma\beta}, \mathbf{q}_{\alpha\gamma}) \oint_{C_+} \frac{d\omega}{2i\pi}$$
$$\Pi^{(ab)}_{SS'}(T_\alpha - \omega - T_\gamma | \mathbf{q}_{\gamma\beta}, \mathbf{q}_{\alpha\gamma}) \otimes \Pi^{(AB)}_{SS'}(\omega | \mathbf{q}_{\gamma\beta}, \mathbf{q}_{\alpha\gamma}) \quad (24)$$

where the expression given in Eq. (13) for the transition potential $\mathcal{U}^{SCE}$ has been used, and projectile and target contributions are contracted to a total spin–scalar reaction amplitude. $T_\alpha = k^2_\alpha/2m_\alpha$ and $T_\gamma = k^2_\gamma/2\bar{m}_\gamma$ denote the kinetic energy in the entrance and intermediate channels, respectively. The energy integral is performed over a closed path C_+ in the upper half complex plane. The products of interaction form factors have been replaced by the spin-spin coupling tensor

$$\Gamma^{(C)}_{SS'}(\mathbf{q}_1, \mathbf{q}_2) = V^{(C)}_{S'T}(q^2_1) V^{(C)}_{ST}(q^2_2). \quad (25)$$

The key quantities are the elements of the nuclear polarization tensor. In Lehmann–representation, they are

$$\Pi^{(AB)}_{SS'}(\omega | \mathbf{q}_1, \mathbf{q}_2) = \sum_C \frac{\langle B | \mathcal{R}_{S'T}(\mathbf{q}_2) | C \rangle \langle C | \mathcal{R}_{ST}(\mathbf{q}_1) | A \rangle}{\omega - (M_C - M_A) + i\eta}, \quad (26)$$

hence given as a bilinear form of the transition form factors, weighted by the energy denominator. $\Pi^{(ab)}_{SS'}$ is defined accordingly. For example, for $|C\rangle = |1^+_n\rangle$ (where n refers to the energy), we find at vanishing momentum transfer

$$\Pi^{(AB)}_{GT}(\omega | \mathbf{q}, \mathbf{q})_{|q=0} = \sum_n \frac{\langle B | \boldsymbol{\sigma}\tau_\pm | 1^+_n \rangle \langle 1^+_n | \boldsymbol{\sigma}\tau_\pm | A \rangle}{\omega - (M_n - M_A) + i\eta}. \quad (27)$$

Comparing this result to the $2\nu2\beta$–NME's, e.g. [33–35], the striking formal analogy is obvious. Of course, there are differences, because here we are dealing with the full momentum structure of the transition currents and their matrix elements. Moreover, the reaction probes at the same time projectile and target NME which requires additional theoretical efforts to disentangle the two kinds of contributions. As a matter of fact, DCE reactions in general are probing a larger part of the nuclear wave functions than ever can be achieved by beta–decay studies. The cross section shown in Fig. 3 covers in the measured angular range momentum transfers $q_{\alpha\beta} \gtrsim 400$ MeV/c – as otherwise expected for $0\nu2\beta$–decay. Moreover, in a DCE transition, several multipolarities can be excited in the intermediate states. From this point of view, DCE reactions can be considered as a perfect test range for scrutinizing nuclear models used in double beta–decay studies.

5. Summary and outlook

Heavy ion double charge exchange reactions have been investigated with the focus on the reaction dynamics of this special class of two-step reactions. The reaction mechanism was described as a double-SCE reaction given by two consecutive SCE reaction steps which are promoted by the projectile-target residual isovector NN-interaction. The DCE reaction amplitude was constructed accordingly as a second order distorted wave matrix element. Broad space was given to disentangle nuclear matrix elements and ion-ion initial and final state interactions.

The DSCE reaction amplitude, Eq. (10), has the formal structure of a matrix element in second order perturbation theory, describing here the next-to-leading-order contribution of the $a + A$ residual isovector interactions. Hence, on the formal level, the DCE amplitude resembles the NME of $2\nu2\beta$ decay. The central message is that DCE reactions cover at the same time dynamical aspects typical for $2\nu2\beta$ but covering a large spectrum of momentum transfers. A consequence of the enhanced momentum content is a non–selectivity on intermediate states: in general, a multitude of intermediate states of both parities and with a large range of spins is excited.

We emphasize that excitations of DCE modes will proceed in general by mixtures of $S = 0$ non-spinflip and $S = 1$ spinflip transitions, thus lifting the strict selection rules known for SCE transitions. One reason is that the final nuclear configurations in projectile and target are of $2p2h$-character with respect to the parent nuclei which allow a broad spectrum of interactions [36]. Thus, the simplicity of SCE reactions, allowing to extract single-beta decay NME from cross section data, is not maintained in the same way for DCE reactions. Accessing DCE-NME's in full detail requires to consider additional observables which are sensitive to the spin-character of the transitions. This does not exclude exceptional, yet to be discovered cases where special configurational properties are enhancing a certain spin channel.

Significant simplifications occur when one considers specific cases, such as $0^+_{gs} \to 0^+_{gs}$ transitions both in projectile and target. Illustrative results have been presented in this case, for the reaction $^{18}O + {}^{40}Ca \to {}^{18}Ne + {}^{40}Ar$, together with a comparison to available experimental data.

DCE processes are determined by many new aspects of nuclear structure and reaction dynamics which have not been under scrutiny until now. Both experiment and theory are entering into hitherto unexplored territory, posing unexpected challenges but opening a new field of nuclear research. In a forthcoming paper, a competing DCE reaction mechanism will be studied of different dynamical origin, as discussed by preliminary results in [14,23]. In [37] a new approach to DCE processes, based on an extended version of the Interacting Boson Model (IBM), was presented. An important message of the present work is that heavy ion DCE reactions are indeed the ideal tools to scrutinize nuclear DCE models under realistic conditions. Our results are encouraging systematic studies in this direction.

Declaration of competing interest

The authors declare that they have no known competing financial interests or personal relationships that could have appeared to influence the work reported in this paper.

Acknowledgements

We wish to thank C. Agodi, F. Cappuzzello and M. Cavallaro for fruitful discussions on experimental methods and results. Partial funding of the INFN-LNS group by the European Union's Horizon 2020 research and innovation program under Grant No. 654002 is acknowledged. J.-A. L. acknowledges support by the Spanish Ministerio de Ciencia, Innovación y Universidades and FEDER funds under project FIS2017-88410-P. H.L. acknowledges gratefully partial support by Alexander von Humboldt Foundation, DFG, grant Le439/16, and INFN.

References

[1] C.H. Dasso, G. Pollarolo, Macroscopic formfactors for pair transfer in heavy ion reactions, Phys. Lett. B 155 (1985) 223–226, https://doi.org/10.1016/0370-2693(85)90642-2.

[2] C.H. Dasso, A. Vitturi, Mechanism for double-charge exchange in heavy ion reactions, Phys. Rev. C 34 (1986) 743–745, https://doi.org/10.1103/PhysRevC.34.743.

[3] J. Blomgren, et al., Search for double Gamow-Teller strength by heavy-ion double charge exchange, Phys. Lett. B 362 (1995) 34–38, https://doi.org/10.1016/0370-2693(95)01190-2.

[4] F. Cappuzzello, et al., Eur. Phys. J. A 54 (2018) 72.
[5] M. Takaki, et al., RIKEN Accel. Prog. Rep. (2013) 47.
[6] H. Lenske, H.H. Wolter, H.G. Bohlen, Phys. Rev. Lett. 62 (1989) 1457.
[7] C. Brendel, P. von Neumann-Cosel, A. Richter, G. Schrieder, H. Lenske, H.H. Wolter, J. Carter, D. Schüll, Nucl. Phys. A 477 (1988) 162–188, https://doi.org/10.1016/0375-9474(88)90367-3.
[8] H.G. Bohlen, et al., Nucl. Phys. A 488 (1988) 89–94, https://doi.org/10.1016/0375-9474(88)90255-2.
[9] H. Lenske, G. Schrieder, Eur. Phys. J. A 2 (1998) 41–53.
[10] N. Auerbach, W.R. Gibbs, J.N. Ginocchio, W.B. Kaufmann, Pion - nucleus double charge exchange and the nuclear shell model, Phys. Rev. C 38 (1988) 1277–1296, https://doi.org/10.1103/PhysRevC.38.1277.
[11] D.L. Watson, et al., Pion induced double charge exchange on C-12, Mg-24, S-32, and Ca-40, Phys. Rev. C 43 (1991) 1318–1320, https://doi.org/10.1103/PhysRevC.43.1318.
[12] M.B. Johnson, C.L. Morris, Pion double charge exchange in nuclei, Annu. Rev. Nucl. Part. Sci. 43 (1993) 165–208, https://doi.org/10.1146/annurev.ns.43.120193.001121.
[13] H. Lenske, J.I. Bellone, M. Colonna, J.A. Lay, Phys. Rev. C 98 (2018) 044620.
[14] H. Lenske, F. Cappuzzello, M. Cavallaro, M. Colonna, Prog. Part. Nucl. Phys. 109 (2019) 103716, https://doi.org/10.1016/j.ppnp.2019.103716.
[15] J.A. Lay, S. Burrello, J.I. Bellone, M. Colonna, H. Lenske, within the NUMEN project, Double charge-exchange reactions and the effect of transfer, J. Phys. Conf. Ser. 1056 (2018) 012029.
[16] S. Burrello, J.I. Bellone, M. Colonna, J.A. Lay Valera, H. Lenske, Springer Proc. Phys. 225 (2019) 177.
[17] F. Cappuzzello, M. Cavallaro, C. Agodi, M. Bondi, D. Carbone, A. Cunsolo, A. Foti, Eur. Phys. J. A 51 (2015) 145, https://doi.org/10.1140/epja/i2015-15145-5, arXiv:1511.03858 [nucl-ex].
[18] C.D. Goodman, et al., Phys. Rev. Lett. 44 (1980) 1755.
[19] F. Osterfeld, Rev. Mod. Phys. 64 (2) (1992) 491–550.
[20] T.N. Taddeucci, et al., Nucl. Phys. A 469 (1987) 125.
[21] D. Frekers, M. Alanssari, Charge-exchange reactions and the quest for resolution, Eur. Phys. J. A 54 (2018) 177, https://doi.org/10.1140/epja/i2018-12612-5.
[22] H. Lenske, J. Phys. Conf. Ser. 1056 (1) (2018) 012030, https://doi.org/10.1088/1742-6596/1056/1/012030.
[23] H. Lenske, in: CERN-Proceedings 2019-001, 2019, pp. 49–56.
[24] G.R. Satchler, Direct Nuclear Reactions, International Series of Monographs on Physics, vol. 68, 1983.
[25] H. Lenske, N. Tsoneva, Eur. Phys. J. A 55 (12) (2019) 238, https://doi.org/10.1140/epja/i2019-12811-6.
[26] N. Tsoneva, H. Lenske, Phys. At. Nucl. 79 (6) (2016) 885, https://doi.org/10.1134/S1063778816060247.
[27] T. Tamura, T. Udagawa, H. Lenske, Phys. Rev. C 26 (1982) 379, https://doi.org/10.1103/PhysRevC.26.379.
[28] H. Lenske, S. Landowne, H.H. Wolter, T. Tamura, T. Udagawa, Phys. Lett. B 122 (1983) 333, https://doi.org/10.1016/0370-2693(83)91576-9.
[29] H. Lenske, H.H. Wolter, A. Weigel, Nucl. Phys. A 690 (2001) 267, https://doi.org/10.1016/S0375-9474(01)00956-3.
[30] M.A. Franey, W.G. Love, Phys. Rev. C 31 (1985) 488.
[31] I.J. Thompson, Comput. Phys. Rep. 7 (1988) 167–212.
[32] F. Cappuzzello, et al., Analysis of the ^{11}B(^{7}Li, ^{7}Be)^{11}Be reaction at 57 MeV in a microscopic approach, Nucl. Phys. A 739 (2004) 30.
[33] T. Tomoda, Double beta-decay, Rep. Prog. Phys. 54 (1991) 53, https://doi.org/10.1088/0034-4885/54/1/002.
[34] A. Bobyk, W.A. Kaminski, J. Phys. G 21 (1995) 229.
[35] F. Šimkovic, A. Smetana, P. Vogel, Phys. Rev. C 98 (6) (2018) 064325, https://doi.org/10.1103/PhysRevC.98.064325, arXiv:1808.05016 [nucl-th].
[36] H. Sagawa, T. Uesaka, Phys. Rev. C 94 (6) (2016) 064325, https://doi.org/10.1103/PhysRevC.94.064325, arXiv:1612.00900 [nucl-th].
[37] E. Santopinto, et al., Phys. Rev. C 98 (2018), 061601 R.